PAPER

NJC
www.rsc.org/njc

The self-assembly switching of the group 13 tetrahedral Schiff base complexes by changing the character of coordination centre

Janusz Lewiński,*[a] Janusz Zachara,[a] Patryk Stolarzewicz,[a] Maciej Dranka,[a] Edyta Kołodziejczyk,[b] Iwona Justyniak[b] and Janusz Lipkowski[b]

[a] *Department of Chemistry, Warsaw University of Technology, Noakowskiego 3 00-664 Warsaw, Poland. E-mail: lewin@ch.pw.edu.pl*
[b] *Institute of Physical Chemistry, Polish Academy of Sciences, Kasprzaka 44/52 01-224 Warsaw, Poland*

Received (in Durham, UK) 26th April 2004, Accepted 28th July 2004
First published as an Advance Article on the web 18th October 2004

The reaction of Et_3B with one equivalent of N-substituted salicylideneimine (HsaldR′) yields the monomeric *O,N*-chelate complexes Et_2B(saldR′), where R′ = Me (**1**) or Ph (**2**). The crystal structure of the resulting complexes has been determined by X-ray crystallography. The molecular structure of these complexes consists of monomeric four-coordinate chelates and their primary arrangement in the crystal structure is determined by the C–H···$O_{aryloxide}$ hydrogen bonds. An extended crystal structure analysis reveals that the adjacent monomeric moieties of **1** are interconnected by C–H_{imino}···O hydrogen bridges resulting in a 1-D motif infinite H-bonded chain, whereas the crystalline complex **2** comprises dimeric molecules linked through a pair of intermolecular C–H_{arom}···O interactions. The supramolecular arrangement of both compounds is discussed with relation to the structure of analogous aluminium and gallium complexes, and the role played by the coordination centre on the molecular assembly is analyzed. It is shown that the steric congestion at the hydrogen bond donor and acceptor sites, as a result of changes in the *N*-alkyl substituents or the coordination centre environment, affect the strength of the intermolecular C–H···O hydrogen bonds and may lead to the self-assembly switching of the bidentate Schiff base complexes.

Introduction

The great potential for producing novel materials with interesting useful functions (with desirable properties) has led to the rational design and synthesis of metal–organic polymeric networks becoming an intensely studied subject. The rational construction of metal–organic supramolecular frameworks involves a cooperation between the metal first-coordination sphere and the second-sphere non-covalent active sites. Schiff bases have been for decades among the most fundamental chelating systems in coordination chemistry, and exploitation of this group of compounds in material science is currently a rapidly developing field.[1] Not surprisingly, recent studies have highlighted the potential importance of hydrogen bonding in tuning the properties of materials based on Schiff base complexes.[1] However, the vast majority of investigations focus on the metal first-coordination sphere of Schiff base complexes, while the ligand frameworks have various donor and acceptor sites capable of participating in an intermolecular hydrogen bond to an adjacent metal-bound ligand, and the fundamental structural consequences exhibited by the second-sphere hydrogen bonding interactions on the reactivity and properties of these type complexes is not a well-developed field. Undoubtedly, the identification of the hydrogen bond preferred mode for Schiff base metal complexes is of fundamental importance in the design of solid-state supramolecules involving this type of ligands and there is considerable current interest in elucidating the role of hydrogen bonding interactions using small-molecule models.

For the last few years we have been engaged in an investigation of relationships between the intra- and intermolecular forces resulting from the donor–acceptor and hydrogen bonding interactions using the group 13 alkoxides[2] and carboxylates[3] as model complexes. These studies have revealed that even minor differences in the subunit structure can have a profound effect on the molecular and crystal structure. An integral part of this work has been to study the structure of group 13 metal alkyl chelate complexes with the salicylideneiminate anion as the *O,N*-bidentate ligand (*M* = Al, Ga and In).[4] The latter complexes were found to be a good basic model system for exploiting the role of hydrogen bonding on the supramolecular structure of Schiff base metal complexes. For instance, the crystal structure analysis of the aluminium and gallium derivatives of *N*-methyl- and *N*-phenyl-salicylideneimine (HsaldPh and HsaldMe, respectively) provided interesting data concerning the effect of *N*-alkyl substituents on the molecular assembly of the tetrahedral chelate complexes. Here we report the structure investigations of the diethylboron derivatives of *N*-phenyl- and *N*-methyl-salicylideneimine, Et_2B(saldR′). In an effort to elucidate factors controlling the supramolecular structure of bidentate Schiff base complexes, we discuss the geometrical parameters of both compounds with relation to the structure of the related aluminium and gallium complexes.

Results and discussion

Synthesis and structure of diethylboron derivatives of N-substituted salicylaldimine

The reaction of Et_3B with one equivalent of N-substituted salicylideneimine (HsaldR′) allows for the isolation of monomeric complexes Et_2B(saldR′) almost quantitatively, where *R*′ = Me (**1**) or Ph (**2**). The resulting compounds were isolated as yellow crystalline solids following evaporation to dryness of the reaction mixture and subsequent recrystallization from hexane/CH_2Cl_2 solution at low temperature. Both compounds

DOI: 10.1039/b406288d

have been characterized in a solution by NMR and IR spectroscopy (see Experimental section) and in the solid state their structures have been determined by X-ray crystallography. The ^{1}H NMR spectra of $Et_2B(saldR')$ shows no complexity and characteristic multiplets of the B–Et protons, the single resonance of N=CH proton, and multiplets of aromatic protons are observed. The ^{11}B NMR spectra consist of a single resonance at 7.6 and 8.9 ppm for **1** and **2**, respectively, corresponding to a four-coordinate boron centre.[5] The IR spectra of **1** and **2** revealed the presence of a strong $\nu_{C=N}$ band of the imine group at 1656 and 1628 cm^{-1}, respectively, which are surprisingly shifted slightly towards higher frequencies with respect to the free ligands values (1640 and 1620 cm^{-1}). Thus, the spectroscopic data are consistent with the monomeric chelate structure of studied complexes.

The solid structures of **1** and **2** comprise, like the corresponding aluminium and gallium derivatives, monomeric species with the extended hydrogen bond network. Compound **1** crystallises in the orthorhombic space group *Pbca*, while **2** shapes monoclinic crystals in *C*2/*c* space group. In an effort to elucidate factors controlling the supramolecular structure of bidentate Schiff base complexes, first we shall focus on the geometrical parameters of **1** and **2** and the related aluminium and gallium complexes of type $Me_2M(saldR')$. The molecular structures of **1** and **2** are shown in Figs. 1 and 2, respectively, while selected interatomic distances and angles are collected in Table 1, together with data obtained previously for the aluminium and gallium analogues.[4] In both structures, the boron centre has a distorted tetrahedral geometry with angles ranging from 93.19(14) to 125.3(3)° and from 104.29(16) to 116.19(19)° in **1** and **2**, respectively. The most acute angle in each case is associated with the bite of the chelating ligand. The six-membered chelate-ring system O(1)C(1)C(2)C(7)N(1)B(1) in **1** is essentially planar (puckering amplitude $Q = 0.137(3)$ Å[6]). In contrast, the analogue heterocycle in **2** is highly deviated from planarity (puckering amplitude $Q = 0.349(2)$ Å) and presents an envelope conformation with B(1) atom displaced 0.486(3) Å out of the almost flat ligand plane. Similar deformations of the chelate ring were observed in the aluminium and gallium derivatives of *N*-phenylsalicylideneimine where the relevant displacement of Al and Ga atoms from the ligand plane is equal 0.250(3) and 0.312(5) Å, respectively. Interestingly, in all cases this deformation is realised by the bending on the aryloxide oxygen atom [the torsion angles M(1)–O(1)–C(1)–C(2) range from −9.3(4) (**1**) to −29.8(3)° (**2**)], while the metal–imine linkage remains essentially planar (the torsion angles M–N=C–C are less than 5°). The B(1)–O(1) distance in compound **1** [1.515(4) Å] is slightly longer, whereas the B(1)–N(1) distance [1.610(4) Å] is shorter, than the corresponding distances in **2** (1.505(3) and 1.642(3) Å, respectively). Undoubtedly, the identity of the *N*-alkyl substituents affect the electronic interactions within the chelate ring which is a significant contributor to the molecular structure of **1** and **2**. The observed B–O and B–N bond lengths are significantly shorter than the M–O and M–N distances in the aluminium and the gallium analogues (Table 1). Nevertheless, these differences are substantially consistent with the increasing covalent radii of boron (0.83 Å), aluminium (1.18 Å) and gallium (1.26 Å). One additional interesting structural feature of the boron complexes is the consistently widened O–B–N angle by comparison to the O–M–N angles for the aluminium (**3**) and gallium (**5**) com-

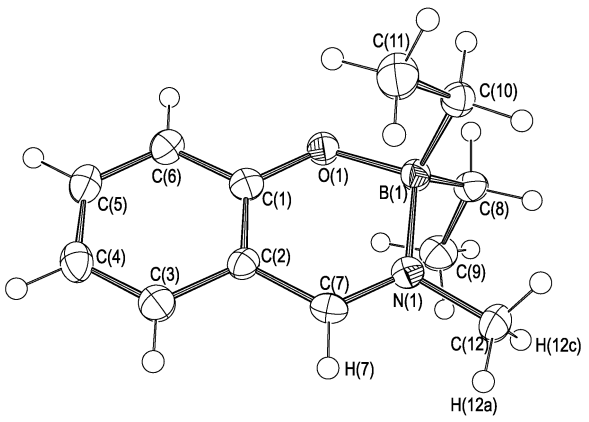

Fig. 1 An ORTEP diagram of molecular structure of $Et_2B(saldMe)$ (**1**) in the solid state showing a 50% probability of thermal ellipsoids.

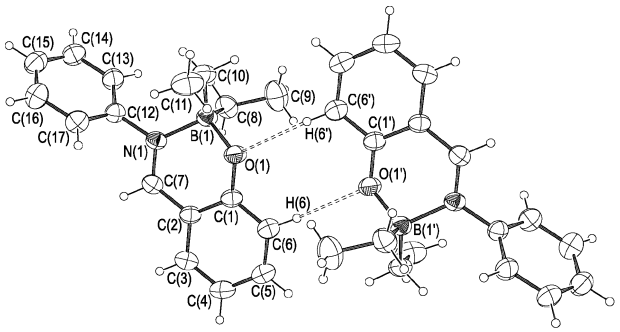

Fig. 2 An ORTEP diagram of hydrogen bonded dimer of Et_2B (saldPh) (**2**) in the solid state showing a 30% probability of thermal ellipsoids. The atoms labelled with a prime (′) are at symmetry equivalent position $(1/2 - x, 1/2 - y, 1 - z)$.

Table 1 Selected bond lengths (Å), bond angles (deg) and torsion angles (deg) for $Et_2B(saldMe)$ (**1**), $Et_2B(saldPh)$ (**2**), $Me_2Al(saldPh)$ (**3**), and $Me_2Ga(saldPh)$ (**5**)

$Et_2B(saldMe)$ (**1**)		$Et_2B(saldPh)$ (**2**)	
B(1)–O(1)	1.515(4)	B(1)–O(1)	1.505(3)
B(1)–N(1)	1.610(4)	B(1)–N(1)	1.642(3)
B(1)–C(8)	1.607(4)	B(1)–C(8)	1.617(3)
B(1)–C(10)	1.617(4)	B(1)–C(10)	1.592(3)
O(1)–C(1)	1.336(3)	O(1)–C(1)	1.332(3)
N(1)–C(7)	1.291(3)	N(1)–C(7)	1.296(2)
C(1)–C(2)	1.405(4)	C(1)–C(2)	1.400(3)
C(2)–C(7)	1.428(4)	C(2)–C(7)	1.429(3)
C(8)–B(1)–C(10)	114.3(2)	C(10)–B(1)–C(8)	116.06(19)
O(1)–B(1)–N(1)	107.1(2)	O(1)–B(1)–N(1)	104.28(16)
C(1)–O(1)–B(1)	124.9(2)	C(1)–O(1)–B(1)	121.71(16)
C(7)–N(1)–B(1)	123.1(2)	C(7)–N(1)–B(1)	120.19(16)
O(1)–C(1)–C(2)	121.4(3)	O(1)–C(1)–C(2)	120.31(18)
C(1)–C(2)–C(7)	119.1(3)	C(1)–C(2)–C(7)	118.52(19)
N(1)–C(7)–C(2)	122.5(2)	C(2)–C(7)–N(1)	122.62(19)
B(1)–O(1)–C(1)–C(2)	−9.3(4)	B(1)–O(1)–C(1)–C(2)	−29.8(3)
B(1)–N(1)–C(7)–C(2)	4.5(4)	B(1)–N(1)–C(7)–C(2)	4.8(4)
		C(17)–C(12)–N(1)–C(7)	55.9(3)

$Me_2Al(saldPh)$ (**3**)[4]		$Me_2Ga(saldPh)$ (**5**)[4]	
Al(1)–O(1)	1.772(2)	Ga(1)–O(1)	1.889(3)
Al(1)–N(1)	1.963(2)	Ga(1)–N(1)	2.023(3)
Al(1)–C(8)	1.943(3)	Ga(1)–C(8)	1.942(5)
Al(1)–C(9)	1.946(3)	Ga(1)–C(9)	1.940(5)
O(1)–C(1)	1.337(3)	O(1)–C(1)	1.324(5)
N(1)–C(7)	1.296(3)	N(1)–C(7)	1.288(5)
C(1)–C(2)	1.402(3)	C(1)–C(2)	1.407(6)
C(2)–C(7)	1.434(3)	C(2)–C(7)	1.432(6)
C(8)–Al(1)–C(9)	119.09(14)	C(8)–Ga(1)–C(9)	125.2(3)
O(1)–Al(1)–N(1)	95.14(9)	O(1)–Ga(1)–N(1)	93.21(14)
C(1)–O(1)–Al(1)	129.71(17)	C(1)–O(1)–Ga(1)	127.1(3)
C(7)–N(1)–Al(1)	121.68(18)	C(7)–N(1)–Ga(1)	122.1(3)
O(1)–C(1)–C(2)	121.6(2)	O(1)–C(1)–C(2)	123.7(4)
C(1)–C(2)–C(7)	123.2(2)	C(1)–C(2)–C(7)	123.7(4)
C(2)–C(7)–N(1)	126.5(3)	C(2)–C(7)–N(1)	127.3(4)
Al(1)–O(1)–C(1)–C(2)	−13.4(4)	Ga(1)–O(1)–C(1)–C(2)	−15.5(7)
Al(1)–N(1)–C(7)–C(2)	0.7(4)	Ga(1)–N(1)–C(7)–C(2)	1.9(7)
C(15)–C(10)–N(1)–C(7)	46.0(4)	C(15)–C(10)–N(1)–C(7)	45.1(6)

Table 2 Selected intermolecular contacts (Å, deg) in **1** and **2**

		1		
C–H···O	C–H	H···O	C···O	C–H···O
C(7)–H(7)···O(1′)[a]	0.95	2.57	3.441(3)	152
C(12)–H(12A)···O(1′)[a]	0.98	2.50	3.438(3)	160
C–H···π	C–H	H···*Cg*[f]	C···*Cg*	C–H···*Cg*
C(12)–H(12C)···π(Ph″)[b]	0.98	3.14	4.031(3)	151
		2		
C–H···O	C–H	H···O	C···O	C–H···O
C(6)–H(6)···O(1′)[c]	0.93	2.54	3.462(3)	171
C–H···π	C–H	H···*Cg*[f]	C···*Cg*	C–H···*Cg*
C(4)–H(4)···π(*N*-Ph″)[d]	0.93	2.82	3.581(3)	140
C(16)–H(16)···π(Ph‴)[e]	0.93	3.10	3.768(4)	130

Symmetry codes:[a] $(-1/2 + x, y, 1/2 - z)$; [b] $(-x, -1/2 + y, 1/2 - z)$; [c] $(1/2 - x, 1/2 - y, 1 - z)$; [d] $(1/2 - x, -1/2 - y, 1\frac{1}{2}-z)$; [e] $(\frac{1}{2} - x, 1\frac{1}{2} - y, 1 - z)$ [f] *Cg*-phenyl ring centroid.

plexes. This is a consequence of the relatively short B–O and B–N distances, and the rigidity of the ligand core. Other bond lengths and angles within the salicylideneiminate ligand of **1** and **2** are typical of such moieties. Furthermore, in regard to the *N*-phenyl complexes, *i.e.* compound **2** and the isostructural Al and Ga complexes, it should be noted the significant twisting of the *N*-phenyl aromatic ring relative to the M–N=C plane. Of the three compounds discussed, in **2** the *N*-phenyl group is twisted towards the chelate ring in the largest degree. The C(17)–C(12)–N(1)–C(7) torsion angle is equal 55.9(3)°, accordingly, it is about 10° larger than in the Al and Ga derivatives.

A detailed inspection of the crystal structures of **1** and **2** revealed that the weak intermolecular hydrogen bond systems play a substantial role in the molecular assembly of crystalline complexes. An analysis of intermolecular contacts showed that adjacent monomeric moieties of **1** are held together in chains by double C–H···O hydrogen bridges. Both the imine hydrogen atom H(7) and the hydrogen atom H(12a) of the methyl group are involved in hydrogen bond interactions with the aryloxide oxygen O(1′) of an adjacent molecule (Table 2). The resulting infinite H-bonded chain is propagated by the *a*-glide plane as depicted in Fig. 3. The length of the glide vector is equal to 6.1205(5) Å. Parallel chains are further interconnected by weak C–H···π(Ph) interactions (dotted lines in Fig. 3) forming grid-like 2-D network on the (001) crystallographic plane. It should be noted that a very similar primary chain structure was recently revealed for the gallium derivative of *N*-methylsalicylideneimine, $Me_2Ga(saldMe)$ (**4**).[4,7] For the latter complex molecules are linked together by the $C–H_{imino}\cdots O_{aryloxide}$ hydrogen bonds and are related by the *c*-glide plane [glide vector equals 6.0343(5) Å]. The secondary structure for this compound is achieved also in a similar way. Chains are assembled by weak C–H···π(Ph) interactions into the 2D double layers lying on the (100) crystallographic plane. Adjacent layers are aligned parallel to each other without interpenetration.

The supramolecular structure of compound **2** is presented in Fig. 4. Surprisingly, it consists of a hydrogen-bonded dimer formed by a pair of adjacent molecules as basic motif. Thus, the observed intermolecular hydrogen bond motif for **2** is entirely different from that found for **1** and the related aluminium and gallium derivatives of *N*-phenylsalicylideneimine, **3** and **5**. The association of the molecular complexes in **2** is attained through a pair of intermolecular $C–H_{arom}\cdots O$ (2.54 Å) interactions between the aryloxide oxygen atom and the hydrogen of the salicylideneimine aromatic ring (Table 2), thus leading to the H-bonded dimer located on the crystallographic centre of symmetry. In addition, the dimeric species are further connected by $C–H_{arom}\cdots\pi$(Ph) interactions to form infinite layers, parallel to the *bc* plane. Both phenyl rings are engaged

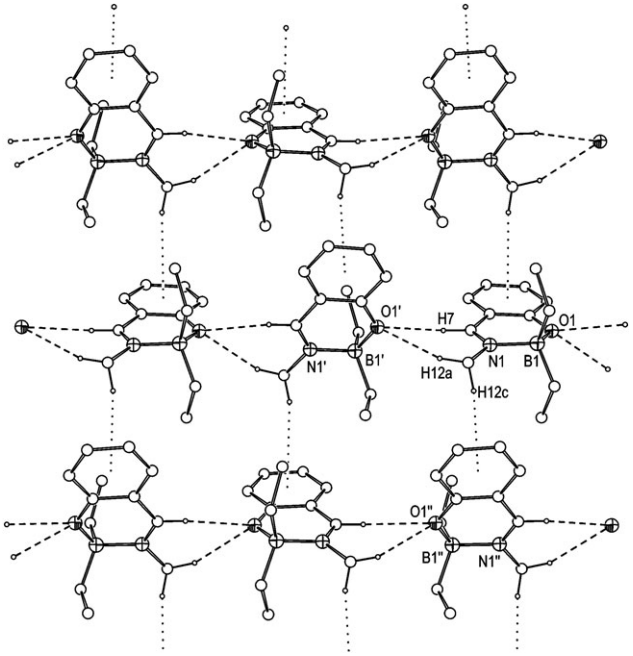

Fig. 3 A view of the 2D hydrogen bonding network in the crystal structure of $Et_2B(saldMe)$ (**1**). The dashed and the dotted lines represent C–H···O and C–H···π(Ph) hydrogen bonds, respectively. Hydrogen atoms are omitted excluding those involved in the H-bond formation.

in the latter interaction. The distances and the angles between the C–H groups and appropriate geometrical centroids of the phenyl rings are included in Table 2. Interestingly, the

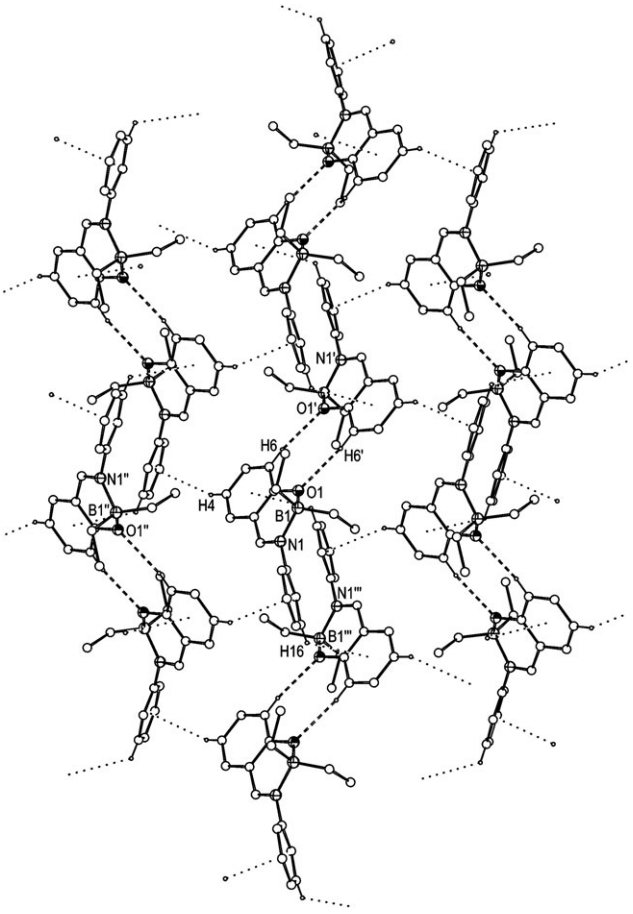

Fig. 4 A view of the 2D hydrogen bonding network in the crystal structure of $Et_2B(saldPh)$ (**2**). The dashed and the dotted lines represent C–H···O and C–H···π(Ph) hydrogen bonds, respectively. Hydrogen atoms are omitted excluding those involved in the H-bond formation.

N═C–H_{imino} hydrogen in **2** is essentially not involved in the hydrogen bond formation (the nearest contact of this proton to the aromatic carbon atom is 3.01 Å).

A Cambridge Structural Database[8] search revealed that up to date only few simple boron Schiff base derivatives of the form $R_2B(O,N)$ have been structurally characterized, all bearing exclusively the diphenylboron moieties.[9–12] Our analysis of the available structure data points that the presence of phenyl groups bonded to the boron centre effectively prevents the association of molecular complexes through intermolecular C–H···O interactions. Instead of the intermolecular hydrogen bonds, both boron bonded phenyl rings, adopting appropriate orientations, are engaged in the intramolecular C–H_{phen}···O or (and) C–H_{phen}···N interactions. The observed H_{phen}···O and H_{phen}···N contacts are equal *ca.* 2.5 and 2.6 Å, respectively.[10–12] However, the crystallization of diphenylboron Schiff base derivative in the presence of the strong H donor, *e.g.* methanol, leads to the formation of a H-bonded solvate.[9]

Toward factors affecting supramolecular structure of bidentate Schiff base metal complexes

The presented above results demonstrate that the molecular structure of $R_2M(saldR')$ (where M = B, Al or Ga) complexes consists of isomorphous monomeric four-coordinate chelate moiety independently of the character of the coordination centre. However, unexpectedly, the crystal structures of these complexes differ significantly. Although in all cases the supramolecular structure is determined by intermolecular hydrogen bonds, the resulting hydrogen bond motifs are distinct. For the boron derivative of *N*-phenylsalicylideneimine, it is the hydrogen-bonded dimer formed by a pair of intermolecular C–H_{arom}···O bridges between the aryloxide oxygen atom and the *ortho*-positioned hydrogen of the salicylideneimine aromatic ring (Scheme 1a). In contrast, for the related aluminium and gallium derivatives of *N*-phenylsalicylideneimine as well as the boron and gallium derivatives of *N*-methylsalicylideneimine, the monomeric moieties are linked by the C–H_{imino}···$O_{aryloxide}$ hydrogen bonds leading to the formation of infinite chain structures (Scheme 1b). Thus, a common feature of the observed hydrogen bond motifs is the aryloxide oxygen acting as the hydrogen acceptor and the difference concerns a competition between the C–H_{imino} and the C–H_{arom} hydrogen donor sites (from the CSD search it appears that the C–H_{imino}···O could be expected as a dominant interaction[13]). In this regard arises the question: why is there a change in the hydrogen bond donor sites in this homologous series of *N*-phenylsalicylideneimine derivatives passing from boron to the heavier group 13 derivatives?

In order to ascertain whether the observed hydrogen bond motifs are determined by the molecular shape, molecular size or other factors, it is instructive to consider the silent features of the molecular structures of $R_2M(saldR')$ complexes. Thus, the relative conformation of the six-membered MOCCCN chelate-ring system appears to be flexible, however one may easily recognise that the extent of the chelate ring deformation is closely related to the geometry of the M–O–C linkage. It is apparent that the change of the M–O–C unit geometry is important in determining the conjugation of the aryloxide oxygen lone pair with the extended π-system of the chelate

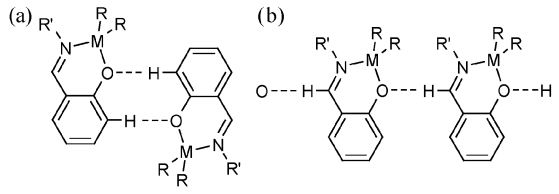

Scheme 1

ring and greatly affect the Lewis basicity of the aryloxide oxygen and may affect the Lewis acidity of potential hydrogen bond donor sites. The planar M–O–C linkage favours the conjugation of the 2pπ nonbonding orbital of the aryloxide oxygen with the π-conjugated ligand bond system and strengthens the stabilization of the oxygen lone pairs. Conversely, the pyramidalisation on the aryloxide oxygen atom strengthens the Lewis basicity of this centre as well as it changes the directionality of the oxygen lone pairs. However, the observed conformational differences between the boron complex and the aluminium and gallium analogues seem to be too small to account for the observed self-assembly switching. Furthermore, the relative orientation of the *N*-phenyl aromatic ring with respect to the M–N═C plane also should affect both the π-conjugation of the *N*-phenyl aromatic ring with the C═N imine group π system and the steric congestion at the N═C–H_{imino} hydrogen, but the observed out-of-plane conformation of the *N*-phenyl ring are not significantly distinct for the complexes in question. So, there must be another effect that influences the hydrogen bond motifs. As was mentioned above, the radius of boron is significantly smaller than that of aluminium and gallium which results in a concomitant decrease in the B–O and B–N bond length. One consequence of this difference is the increase of steric congestion at the aryloxide oxygen in **2**. The formation of the C–H_{imino}···$O_{aryloxide}$ hydrogen bond chains requires a relatively close approach of the –(Ph)N═C–H_{imino} hydrogen to the metal bonded aryloxide oxygen which in the case of boron complex causes a more significant repulsion between the phenyl ring and the sterically congested Et_2BO tetrahedron face. Thus, in our opinion the different preference of the C–H donor sites for the intermolecular hydrogen bonding is dominantly due to the different steric congestion of the Et_2BON core in **2** as compared to the Me_2MON core in the related heavier group 13 derivatives of *N*-phenylsalicylideneimine, and it could affect the strength of the C–H···O hydrogen bond in the solid state. In turn, a considerably greater congestion in the structure based on the C–H_{imino}···$O_{aryloxide}$ hydrogen bond promotes the formation of the double hydrogen bond dimer, where the cooperative C–H_{arom}···O interactions sufficiently compete with the chain array of C–H···O bonds involving the stronger hydrogen bond donor site. It should also be emphasised that additional hydrogen bond formations are observed in these complexes which undoubtedly support the basic hydrogen bond motifs. For instance, the hydrogen-bonded dimers of **2** are further connected by C–H_{arom}···π(Ph) interactions which lead to the formation of infinite layers.

Further support for the assumption that steric congestions at the hydrogen donor and acceptor sites strongly affect the supramolecular structure of tetrahedral complexes stabilized by monoanionic bidentate Schiff base ligands is provided by the comparison of the crystal structure of the aluminium and gallium derivatives of *N*-methyl- and *N*-phenyl-salicylideneimine, $Me_2M(saldPh)$ and $Me_2M(saldMe)$ complexes. The molecular structure of these complexes consists of isostructural monomeric four-coordinate chelates and their primary arrangement in the crystal structure is determined by the C–H_{imino}···$O_{aryloxide}$ hydrogen bonds. However, the replacement of the *N*-methyl to *N*-phenyl group in the bidentate salicylideneiminate ligand leads to significant changes in the molecular assembly. The gallium complex **4** with the *N*-methyl ligand forms the C–H_{imino}···$O_{aryloxide}$ hydrogen bonded molecular chains (*vide supra*). On the other hand, for the *N*-phenyl complexes **3** and **5**, the monomeric moieties related by 4_1 (4_3) screw axis are linked by the C–H_{imino}···$O_{aryloxide}$ hydrogen bonds which lead to the formation of infinite helices as depicted in Fig. 5.[4] The parallel alternating left- and right-handed helical chains are further joined by C–H···π(Ph) interactions to form a tetragonal net. Except for the slightly different ionic radii of aluminium and gallium, the two

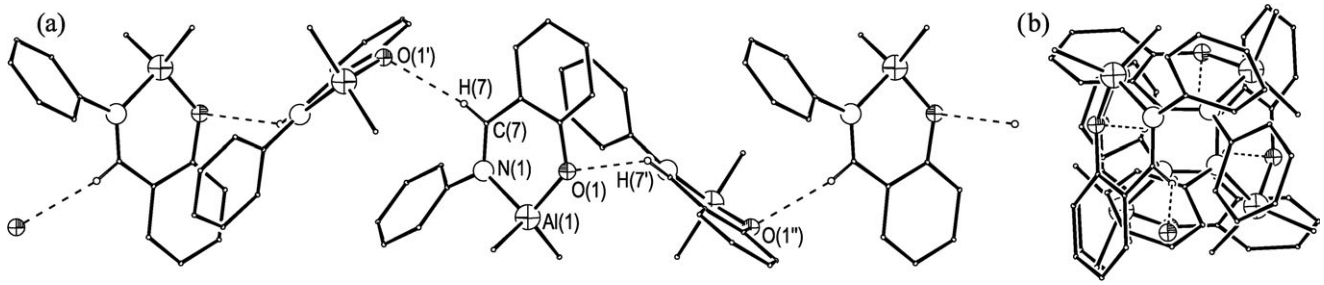

Fig. 5 (a) A view of the helical chain structure of $Me_2Al(saldPh)$ (**3**). (b) A view of the molecular helix along *c* axis. The dashed lines represent C–H···O hydrogen bonds. Hydrogen atoms are omitted excluding those involved in H-bond formation.

complexes are isostructural which indicates that in this case the metal centre does not exert a significant influence on the molecular assembly. So, there appears that small differences in the molecular shape of $Me_2M(saldPh)$ and $Me_2M(saldMe)$ complexes alter the mode of the molecular assembly in the solid state. To compare, the *N*-methyl complex possesses a relatively uncongested environment at the N=C–H hydrogen, while in the *N*-phenyl complex the considerably greater steric congestion imposed by the imine ligand may be responsible for the observed switch in the molecular assembly. This change in the steric congestion at the N=C–H hydrogen appears to greatly affect the spatial arrangement of the component molecules and to change the hydrogen bonding pattern.

In conclusion, while the group 13 compounds $R_2M(saldR')$ complexes exist in the solid state as isostructural monomeric four-coordinate chelate species, small differences in the molecular shape and molecular size significantly affect their crystal structure. Two basic hydrogen bond motifs are observed for this group of complexes: the hydrogen-bonded dimer formed by a pair of intermolecular $C–H_{arom}\cdots O$ interactions between the aryloxide oxygen atom and the *ortho*-positioned hydrogen of the salicylideneimine aromatic ring, and the array of the $C–H_{imino}\cdots O_{aryloxide}$ hydrogen bonds leading to the formation of infinite chains. Thus, a common feature of the hydrogen bond motifs is the aryloxide oxygen acting as the hydrogen acceptor and the difference concerns a competition between the $C–H_{imino}$ and the $C–H_{arom}$ hydrogen donor sites. The analysis of the structural parameters of $R_2M(saldR')$ complexes indicates that the steric congestion at the hydrogen bond donor and acceptor sites, as a result of changes in the *N*-alkyl substituents or the coordination centre environment, affect the strength of the internal C–H···O hydrogen bond and may lead to self-assembly switching of the bidentate Schiff base metal complexes.

Experimental

All operations were carried out under dry nitrogen using standard Schlenk techniques. Solvents and reagents were purified and dried by standard techniques. NMR spectra were recorded on a Varian Mercury (400 MHz) spectrometer in $CDCl_3$ solutions. The IR spectra were recorded on a Specord M80 spectrophotometer in CH_2Cl_2 solutions.

$Et_2B(saldMe)$ (1). A solution of *N*-methylsalicylideneimine (0.52 g, 3.85 mmol) in toluene (5 mL) was cooled to −78 °C, and Et_3B (0.56 cm^3, 3.85 mmol) was added dropwise. After the addition was completed, the reaction mixture was warmed to room temperature and stirred for 24 h, then the volatiles were removed *in vacuo*. The resulting complex was obtained as yellow oil. Yellow crystals were obtained after crystallization from pentane solution at −15 °C. Anal. Calcd for $C_{12}H_{18}BNO$: C, 70.97; H, 8.93; N, 6.90. Found: C, 70.74; H, 9.21; N, 6.22. ^1H NMR ($CDCl_6$): δ 0.48 (q, 4H, B–CH_2), 0.84 (*t*, 6H, CH_3–CH_2),), 3.21 (s, 3H, N–CH_3), 6.6 – 7.4 (m, 4H, Ar*H*), 7.85 (s, 1H, *CH*=N). ^1B NMR ($CDCl_3$): δ 7.6. IR (cm^{-1}): 456(m), 524(w), 596(w), 704(w), 812(m), 928(s), 968(m), 1012(m), 1056(m), 1068(m), 1124(m), 1152(s), 1232(m), 1316(s), 1336(m), 1392(m), 1420(m), 1436(m), 1460(s), 1480(s), 1540(m), 1560(m), 1608(s), 1656(vs), 2824(m), 2868(m), 2908(m), 2948(m).

$Et_2B(saldPh)$ (2). A solution of *N*-phenylsalicylideneimine (0.43 g, 2.18 mmol) in toluene (6 mL) was cooled to –78 °C, and Et_3B (0.32 cm^3, 2.18 mmol) was added dropwise. After the addition was completed, the reaction mixture was warmed to room temperature and stirred for 1.5 h, then the volatiles were removed *in vacuo*. Complex **1a** was obtained as yellow crystals after a recrystallization from hexane/CH_2Cl_2 solution at 5 °C. Anal. Calcd for $C_{17}H_{20}BNO$: C, 77.00; H, 7.60; N, 5.28. Found: C, 76.84; H, 7.76; N, 5.06. ^1H NMR ($CDCl_3$): δ 0.51 (q, 4H, B–CH_2), 0.76 (*t*, 6H, CH_3–CH_2), 6.7–7.5 (m, 9H, Ar*H*), 8.00 (s, 1H, C*H*=N). ^{11}B NMR ($CDCl_3$): δ 8.9. IR (cm^{-1}): 456(m), 556(m), 692(m), 724(m), 784(m), 808(m), 896(m), 920(m), 944(m), 1012(m), 1028(m), 1056(m), 1068(m), 1128(m), 1152(m), 1200(s), 1240(m), 1320(m), 1340(m), 1376(m), 1420(m), 1436(m), 1460(m), 1476(m), 1492(m), 1508(m), 1552(s), 1596(m), 1628(vs), 2868(m), 2908(m), 2952(m).

Table 3 X-ray data collection and structure refinement parameters for compounds **1** and **2**†

	$Et_2B(saldMe)$ (**1**)	$Et_2B(saldPh)$ (**2**)
Formula	$C_{12}H_{18}BNO$	$C_{17}H_{20}BNO$
M	203.08	265.15
Temperature/ K	100(2)	293(2)
Crystal system	Orthorhombic	Monoclinic
Space group	*Pbca* (no. 61)	*C*2/*c* (no. 15)
Radiation	Mo-Kα (λ = 0.7107 Å)	
a/Å	12.2407(9)	22.3787(8)
b/Å	13.557(2)	10.7423(6)
c/Å	14.531(2)	15.2876(9)
β/°	90	123.090(2)
U/Å^3	2411.4(5)	3079.1(3)
Z	8	8
D_c/g cm^{-3}	1.119	1.144
μ/ mm^{-1}	0.069	0.069
F(000)	880	1136
Crystal size/ mm	0.18 × 0.22 × 0.24	0.15 × 0.20 × 0.30
2θ Range/°	5.3 to 45.0	5.4 to 50.0
Independent refls (R_{int})	1567 (0.060)	2702 (0.051)
Data, restraints, param.	1567, 0, 140	2702, 0, 184
Goodness of fit on F^2	1.077	1.033
*R*1, *wR*2 [$I > 2\sigma(I)$][a]	0.0552, 0.1009	0.0481, 0.1070
*wR*2 (all data)	0.112	0.134
Weights *a*, *b*[b]	0.0366, 0.885	0.0557, 0
Extinction coeff. χ[c]	0.0059(9)	0.0077(8)
Max, min $\Delta\rho$/e Å^{-3}	+0.154/−0.164	+0.125/−0.102

[a] $R1 = \Sigma||F_o| - |F_c||/\Sigma|F_o|$, $wR2 = [\Sigma w(F_o^2 - F_c^2)^2/\Sigma w(F_o^4)]^{1/2}$; [b] $w = 1/[\sigma^2(F_o^2) + (a \cdot P)^2 + b \cdot P]$, where $P = (F_o^2 + 2F_c^2)/3$. [c] $F_c^* = kF_c[1 + 0.001 \cdot \chi \cdot F_c^2\lambda^3/\sin(2\theta)]^{-1/4}$, where *k* = overall scale factor.

† CCDC reference numbers [CCDC NUMBER(S)]. See http://www.rsc.org/suppdata/nj/b4/b406288d/ for crystallographic data in .cif or other electronic format.

X-ray crystallography

Single crystals of **1** and **2** suitable for X-ray diffraction studies were placed in a thin walled capillary tubes (Lindemann glass) in an inert atmosphere, plugged with grease and flame sealed. X-ray diffraction data were collected on a Nonius Kappa-CCD diffractometer. Crystal data, data collection and refinement parameters are given in Table 3. The data were corrected for Lorentz-polarization effects. The crystal structures were solved by direct methods using the SHELXS-86 program.[14] Full-matrix least-squares refinement method against F^2 values was carried out by using the SHELXL-97.[15] All non-hydrogen atoms were refined with anisotropic displacement parameters. The hydrogen atoms were introduced at geometrically idealized coordinates with a fixed isotropic displacement parameter equal to 1.2 or 1.5 (methyl groups) times the value of the equivalent isotropic displacement parameter of the parent carbon. An extinction correction was applied for both data sets during the final stages of refinement. The final Fourier-difference maps have no significant chemical meaning. Computations for the crystal structure discussions were carried out with the PLATON program.[16] ORTEP drawings were made using ORTEP3 for Windows.[17]

Acknowledgements

We thank the State Committee for Scientific Research (Grant No. 4 T09A 165 23) for support.

References

1 For recent examples see: (*a*) M. S. Ray, A. Ghosh, R. Bhattacharya, G. Mukhopadhyay, M. G. B. Drew and J. Ribas, *J. Chem. Soc., Dalton Trans*., 2004, 252; (*b*) S. Mizukami, H. Houjou, Y. Nagawa and M. Kanesato, *Chem. Commun*., 2003, 1148; (*c*) I. Ratera, D. Ruiz-Molina, J. Vidal-Gancedo, J. J. Novoa, K. Wurst, J. F. Letard, C. Rovira and J. Veciana, *Chem.-Eur. J*., 2004, **10**, 603; (*d*) A. J. Gallant and M. J. MacLachlan, *Angew. Chem.-Int. Edit*., 2003, **42**, 5307; (*e*) P. G. Cozzi, L. S. Dolci, A. Garelli, M. Montalti, L. Prodi and N. Zaccheroni, *New J. Chem*., 2003, **27**, 692; (*f*) G. K. Patra and I. Goldberg, *New J. Chem*., 2003, **27**, 1124.

2 (*a*) J. Lewiński, J. Zachara and K. B. Starowieyski, *J. Chem. Soc., Dalton Trans*., 1997, 4217; (*b*) J. Lewiński, J. Zachara, T. Kopeć, K. B. Starowieyski, J. Lipkowski, I. Justyniak and E. Kołodziejczyk, *Eur. J. Inorg. Chem*., 2001, 1123; (*c*) J. Lewiński, J. Zachara and I. Justyniak, *Organometallics*, 1997, **16**, 4597; (*d*) J. Lewiński, J. Zachara and I. Justyniak, *Chem. Commun*., 2002, 1586; (*e*) J. Lewiński, J. Zachara, P. Horeglad, D. Glinka, J. Lipkowski and I. Justyniak, *Inorg. Chem*., 2001, **40**, 6086.

3 (*a*) J. Lewiński, J. Zachara and I. Justyniak, *Inorg. Chem*., 1998, **37**, 2575; (*b*) J. Lewiński, I. Justyniak, J. Lipkowski and J. Zachara, *Inorg. Chem., Commun*., 2000, **3**, 700; (*c*) C. S. Branch, J. Lewiński, I. Justyniak, S. G. Bott, J. Lipkowski and A. R. Barron, *J. Chem. Soc., Dalton Trans*., 2001, 1253.

4 J. Lewiński, J. Zachara, K. B. Starowieyski, Z. Ochal, I. Justyniak, T. Kopeć, P. Stolarzewicz and M. Dranka, *Organometallics*, 2003, **22**, 3773.

5 J. Lewiński, in *Encyclopedia of Spectroscopy and Spectrometry*, eds. J. C. Lindon, G. E. Tranter and J. L. Holmes, Academic Press, New York, Vol. 1, 1999, pp. 691–703.

6 D. Cremer and J. A. Pople, *J. Am. Chem. Soc*., 1975, **97**, 1354.

7 (*a*) V. I. Bregadze, N. G. Furmanova, L. M. Golubinskaya, O. Y. Kompan, Yu. T. Struchkov, V. A. Bren, Zh. V. Bren, A. E. Lyubarskaya, V. I. Minkin and L. M. Sitkina, *J. Organomet. Chem*., 1980, **192**, 1; (*b*) The refinement of the structure of 4 was only performed for non-hydrogen atoms. In order to analyse intermolecular interactions H-atoms were introduced in the calculated positions (PLATON[16]).

8 The CSD 3D Graphics Search System v5.25 (November 2003): F. H. Allen, *Acta Crystallogr., Sect. B*, 2002, **58**, 380.

9 BONBAH, R. Allmann, E. Hohaus and S. Olejnik, *Z. Naturforsch., B: Chem. Sci*., 1982, **37**, 1450.

10 LEKQUN, H. Hopfl and N. Farfan, *Can. J. Chem*., 1998, **76**, 1853.

11 MONALB, O. E. Kompan, N. G. Furmanova, Yu. T. Struchkov, L. M. Sitkina, V. A. Bren and V. I. Minkin, *Zh. Strukt. Khim*., 1980, **21**, 90.

12 REVQUE, D. A. Atwood, J. A. Jegier, M. P. Remington and D. Rutherford, *Aust. J. Chem*., 1996, **49**, 1333.

13 J. Lewiński, J. Zachara, I. Justyniak and M. Dranka, *Coord. Chem. Rev*., submitted for publication.

14 G. M. Sheldrick, *Acta Crystallogr., Sect. A*, 1990, **46**, 467.

15 G. M. Sheldrick, *SHELXL-97, Program for Crystal Structure Refinement*, University of Göttingen, Göttingen, Germany, 1997.

16 (*a*) A. L. Spek, *PLATON, A Multipurpose Crystallographic Tool*, Utrecht Univ., Utrecht, The Netherlands, 2002; (*b*) A. L. Spek, *J. Appl. Crystallogr*., 2003, **36**, 7.

17 L. J. Farrugia, *J. Appl. Crystallogr*., 1997, **30**, 565.